

Contents lists available at [SciVerse ScienceDirect](http://www.sciencedirect.com)

## Biomaterials

journal homepage: [www.elsevier.com/locate/biomaterials](http://www.elsevier.com/locate/biomaterials)

## Mitigation of diabetes-related complications in implanted collagen and elastin scaffolds using matrix-binding polyphenol

James P. Chow<sup>a</sup>, Dan T. Simionescu<sup>a</sup>, Harleigh Warner<sup>a</sup>, Bo Wang<sup>b</sup>, Sourav S. Patnaik<sup>b</sup>, Jun Liao<sup>b</sup>, Agneta Simionescu<sup>a,\*</sup>

<sup>a</sup>Biocompatibility and Tissue Regeneration Laboratory, Department of Bioengineering, Clemson University, Clemson, SC 29634, USA

<sup>b</sup>Tissue Bioengineering Laboratory, Department of Agricultural & Biological Engineering, Mississippi State University, Mississippi State, MS 39762, USA

## ARTICLE INFO

## Article history:

Received 25 September 2012

Accepted 30 September 2012

Available online xxx

## Keywords:

AGE

Antioxidant

Matrix proteins

Vascular graft

Heart valve

## ABSTRACT

There is a major need for scaffold-based tissue engineered vascular grafts and heart valves with long-term patency and durability to be used in diabetic cardiovascular patients. We hypothesized that diabetes, by virtue of glycoxidation reactions, can directly crosslink implanted scaffolds, drastically altering their properties. In order to investigate the fate of tissue engineered scaffolds in diabetic conditions, we prepared valvular collagen scaffolds and arterial elastin scaffolds by decellularization and implanted them subdermally in diabetic rats. Both types of scaffolds exhibited significant levels of advanced glycation end products (AGEs), chemical crosslinking and stiffening –alterations which are not favorable for cardiovascular tissue engineering. Pre-implantation treatment of collagen and elastin scaffolds with penta-galloyl glucose (PGG), an antioxidant and matrix-binding polyphenol, chemically stabilized the scaffolds, reduced their enzymatic degradation, and protected them from diabetes-related complications by reduction of scaffold-bound AGE levels. PGG-treated scaffolds resisted diabetes-induced crosslinking and stiffening, were protected from calcification, and exhibited controlled remodeling in vivo, thereby supporting future use of diabetes-resistant scaffolds for cardiovascular tissue engineering in patients with diabetes.

Published by Elsevier Ltd.

### 1. Introduction

Diabetes, one of the major risk factors for cardiovascular disease (CVD), is increasing to epidemic proportions worldwide; currently it affects 8% of the world's population and nearly 26 million people in US alone [1]. Hyperglycemia, resulting from the deficiency in insulin secretion (Type 1 diabetes) or insulin resistance (Type 2 diabetes), combined with dyslipidemia, oxidative stress, and inflammation, significantly increases the risk of atherosclerotic vascular disease [2], aortic valve disease [3,4] and cardiomyopathy [5]. Studies have shown that, despite great advances in diagnosis and treatment of CVD, over the last several years diabetic patients have not shared the same decline in coronary artery disease-related mortality as non-diabetic patients [2].

The primary cause of cardiovascular tissue damage occurring in diabetes is the formation of advanced glycation end products

(AGEs), which generate irreversible cross-links on long-lived proteins, such as collagen and elastin [6,7]. Glucose and lipid molecules undergo a series of oxidant-induced fragmentation, leading to the formation of short-chain reactive compounds that react with proteins and form AGEs, such as carboxy-methyl lysine (CML) and pentosidine [8]. Malondialdehyde (MDA) is a marker for oxidative stress and a well known by-product of lipid peroxidation [9]. AGEs impair wound healing and induce excessive inflammation [10], fibrosis, and tissue stiffness [11–13]. As a result, the outcome of reparative surgery and tissue transplantation is more problematic in diabetic patients [14].

Tissue engineering holds great promise to treat cardiovascular diseases [15,16]. Significant progress has been made in the field of blood vessel [17–19], heart valve [20,21] and cardiac tissue engineering [22,23]. It is critical that replacements for damaged cardiovascular structures possess appropriate biomechanical properties from the outset of implantation. Therefore, there is increased interest in collagen and elastin-based biological scaffolds derived from xenogeneic or allogeneic extracellular matrices (ECM), which have optimal physical properties. Furthermore, the 3D structure of the ECM can be preserved with an optimal decellularization technique that removes cells without damaging the

\* Corresponding author. Department of Bioengineering, 201 Rhodes Research Center, Clemson University, Clemson, SC 29634, USA. Tel.: +1 864 656 3729; fax: +1 864 656 4466.

E-mail address: [agneta@clemson.edu](mailto:agneta@clemson.edu) (A. Simionescu).

matrix components [24–26]. Ideally, basement membrane proteins are also retained, as their presence is essential to tissue regeneration [27].

For pre-clinical evaluation, tissue engineered constructs and their remodeling are typically tested in healthy animals [28–30]. However, there are great expectations that TE and regenerative medicine research will offer solutions for patients affected by the cardiovascular complications of diabetes. The complex glyco-oxidative environment could affect tissue remodeling since the ECM proteins, especially collagen and elastin as well as the matrix metalloproteinases (MMPs) involved in matrix remodeling, might be modified by the formation of AGEs. Matrix alterations that result in activation of inflammation, fibrosis, and impaired healing might not be conducive to the desired integration and remodeling of tissue engineered constructs. These aspects can only be assessed in diabetic animal models with very strict glycemic control [31–33].

Polyphenols, which are based on gallic acid units bound to a polyol core exhibit high affinity for proline-rich proteins [34], particularly to collagen [35] and elastin [36,37]. Penta-galloyl glucose, (PGG) a well-characterized polyphenol [38], can increase the stability of collagen and elastic scaffolds and slow down their degradation [25,35]. PGG has been reported to have many beneficial effects such as antioxidant, antidiabetic, and anti-inflammatory activities [39].

We hypothesized that AGEs could alter the properties of matrix-derived scaffolds, such as collagen scaffolds used for heart valve tissue engineering and elastin scaffolds for blood vessel tissue engineering. This could affect the outcome of tissue engineering products based on biological scaffolds. Polyphenols, by virtue of their antioxidant properties and collagen- and elastin-binding abilities, might protect the structural matrix proteins from diabetes-related complications. Therefore, we used a diabetic rat model and implanted PGG-treated scaffolds subdermally for four weeks. Scaffolds were then removed and analyzed for their mechanical and biochemical properties.

## 2. Materials and methods

### 2.1. Materials

High-purity penta-galloyl glucose was a generous gift from N.V. Ajinomoto OmniChem S.A., Wetteren, Belgium ([www.omnichem.be](http://www.omnichem.be)). Streptozotocin was from Sigma (S0130). The insulin preparation used for rats in this study was Humulin N U-100 NPH, Human Insulin of rDNA origin Isophane suspension from Lilly (Indianapolis, IN). Electrophoresis apparatus, chemicals, and molecular weight standards were from Bio-Rad (Hercules, CA). Bicinchoninic acid protein assay kit was from Pierce Biotech (Rockford, IL). The Vectastain Elite kit and the ABC diaminobenzidine tetrahydrochloride peroxidase substrate kit were purchased from Vector Laboratories (Burlingame, CA). We used the following antibodies: rabbit anti-collagen IV (Abcam, #ab6586), rabbit anti-laminin (Abcam, #ab11575), monoclonal anti-N-epsilon-(carboxymethyl)lysine (CML) antibody (MAB3247, R&D Systems), monoclonal anti-vimentin (V5255, Sigma), mouse anti-CD8 (GTX76218, GeneTex Inc, Irvine, CA), mouse anti-CD68 anti-macrophage/monocyte antibody, clone ED-1 (MAB1435, Millipore, Billerica, MA). Deoxyribonuclease I was from Worthington Biochemical Corporation (Lakewood, NJ). AlphaTRAK (Gen II) test strip and the AlphaTRAK® Blood Glucose Monitoring System was from Abbott Laboratories, Animal Health (Abbott Park, IL). All other chemicals were of highest purity available and were obtained from Sigma–Aldrich Corporation (Lakewood, NJ).

### 2.2. Heart valve collagen scaffold preparation

Collagen scaffolds were prepared following a protocol described previously with minor modifications [26]. Briefly, fresh porcine aortic roots were harvested from a local slaughterhouse, cleaned over ice, and placed in double-distilled water overnight at 4 °C to induce hypotonic shock and cell lysis. Next, for complete cell removal, the valves were placed on an orbital shaker at room temperature and treated with the 0.05M NaOH for 2 h followed by 70% ethanol for 20 min and an overnight incubation in a mixture of detergents: 0.5% sodium dodecyl sulfate, 0.5% Triton X-100, 0.5% deoxycholate, 0.2% ethylenediaminetetra-acetic acid in 50 mM TRIS, pH7.5. After rinsing five times with double-distilled water and 70% ethanol to remove detergents, valves were treated with deoxyribonuclease/ribonuclease

mixture (360mU/ml for each enzyme) for 2 days at 37 °C, to complete the removal of nucleic acids. After rinsing with double-distilled water, valves were sterilized in 70% ethanol overnight at room temperature. Under sterile conditions, the aortic cusps were dissected away from the aortic wall and stored in sterile ddH<sub>2</sub>O with 1% antibiotic/antimycotic (Pen-Strep) at 4 °C. Each individual cusp served as a collagen scaffold. This decellularization method effectively removed cells, while preserving valve matrix components and eliminating the porcine  $\alpha$ -Gal epitope [26].

### 2.3. Arterial elastin scaffold preparation

Elastin scaffolds were prepared following an alkaline extraction protocol described before, with minor modifications [25]. Briefly, fresh porcine carotid arteries (60–80 mm long, 5–6 mm in diameter) obtained from Animal Technologies, Inc. (Tyler, TX) were rendered acellular by incubation in 0.1M NaOH solution at 37 °C for 24 h followed by extensive rinsing with deionized water until pH dropped to neutral. Scaffolds were then rinsed and stored in sterile PBS. This treatment removed all cells and most of the collagen, leaving vascular elastin intact. Scaffolds were also completely devoid of the  $\alpha$ -Gal epitope (data not shown).

### 2.4. PGG-treatment of scaffolds

The acellular scaffolds were treated with sterile 0.1% PGG in 50 mM 4-(2-hydroxyethyl)-1-piperazineethanesulfonic acid (HEPES) solution in saline (pH 5.5) containing 20% isopropanol overnight at room temperature under agitation and protected from light. Scaffolds were then rinsed in sterile PBS and stored in sterile PBS containing 1% protease inhibitor and 1% Pen-Strep at 4 °C. The efficiency of PGG binding and tissue stabilization was assessed previously by testing tissue resistance to collagenase and elastase digestion [25,26]. Untreated acellular scaffolds were used as controls.

### 2.5. Rat model of STZ-induced diabetes

Adult male Sprague–Dawley rats ( $n = 40$ , weight 300–350 g) were rendered diabetic via a single dose of sterile filtered 55 mg/kg streptozotocin solution in 0.1M citrate buffer (pH 5) by tail vein injection. Control rats ( $n = 40$ ) received an equal volume of vehicle (sterile citrate buffer). Starting on day 3, levels of blood glucose were determined 3–4 times per week, using AlphaTRAK (Gen II) test strips on the AlphaTRAK Blood Glucose Monitoring System, designed specifically for animals. Diabetes was established (>400 mg glucose/dL blood), and diabetic rats were given subcutaneous injections of long-lasting insulin (2-4U Isophane) every other day to maintain blood glucose level in a desirable range (400–600 mg glucose/dL blood) and prevent development of ketonuria and weight loss. Glucose levels, individual weights, hydration status, and food and water consumption were monitored closely and continuously graphed to ensure adequate health parameters. Animals were provided with food and water *ad libitum* and were cared for by the attending university veterinarian and associated staff at the Godley-Snell Research Center animal facility. The Animal Research Committee at Clemson University approved the animal protocol, and National Institute of Health (NIH) guidelines for the care and use of laboratory animals (NIH publication #86-23 Rev. 1996) were observed throughout the experiment.

### 2.6. Experimental implant groups

Scaffolds were divided into four groups as follows: a) non-treated collagen scaffolds; b) PGG-treated collagen scaffolds; c) non-treated elastin scaffolds; d) PGG-treated elastin scaffolds. Samples from each group were implanted subdermally into control and diabetic rats ( $n = 20$  implants per group) as detailed below.

### 2.7. Subdermal implantation

Four weeks after STZ administration, rats were prepped for surgery and anesthetized using 1–2% Isoflurane. A small, transverse incision was made on the back of the rats, and two subdermal pouches were created by blunt dissection. The acellular scaffolds were implanted – one whole acellular aortic cusp (collagen scaffold) in each pocket ( $n = 2$  implants per rat), and the incision was closed with surgical staples. Acellular arteries (elastin scaffolds) were cut open longitudinally and  $1 \times 3$  cm samples were implanted subdermally, as described above for cusps ( $n = 2$  per rat). Diabetic rats were given 1U of insulin pre-operatively. The rats were allowed to recover, provided with food and water *ad libitum*, and were cared for by the attending veterinarian and associated staff at the Godley-Snell Research Center animal facility. Post-operative levels of blood glucose were determined 3–4 times per week, and diabetic rats were given insulin as described above. After four weeks, the rats were humanely euthanized by CO<sub>2</sub> asphyxiation and the scaffolds explanted and collected according to their respective assay application as follows: scaffolds for histological analysis were placed in Karnovsky's Fixative (2.5% glutaraldehyde, 2% formalin, 0.1M cacodylic acid, pH 7.4) and paraffin embedded; samples designated for mechanical analysis were collected in sterile PBS with 0.02% Na<sub>3</sub>N; and samples for protein, calcium and AGE analysis were flash frozen in liquid nitrogen and kept on dry ice until transferred to –20 °C for storage.



## 2.8. Histological analysis

Rehydrated paraffin sections (5  $\mu\text{m}$ ) were stained with Hematoxylin and Eosin (H&E) for a general overview of morphology and to confirm cellular removal. Movat's Pentachrome stain was used to evaluate the extracellular matrix composition and integrity after decellularization and after implantation ( $n = 4$  per implant group).

Immunohistochemistry (IHC) was performed for detection of laminin and type IV collagen in acellular scaffolds, and the results were compared to native cusps and arteries ( $n = 4$  per implant group). Briefly, rehydrated paraffin sections (5  $\mu\text{m}$ ) were exposed to 0.1% Proteinase K in 10 mM TRIS buffer, pH7.5, at room temperature for 30 s to unmask the antigens. Endogenous peroxidases were blocked with 0.3% hydrogen peroxide in 0.3% horse normal serum. Sections were treated with 0.025% Triton X-100 for 10 min and then incubated with normal blocking serum for 20 min. Primary antibodies (rabbit anti-laminin, 4  $\mu\text{g}/\text{mL}$  dilution, or rabbit anti-collagen type IV, 2  $\mu\text{g}/\text{mL}$  dilution) were applied for 1 h at room temperature. Negative staining controls were obtained by the omission of the primary antibody. The Vector ABC peroxidase substrate kit was then used to visualize the antibody staining, and sections were lightly counterstained with Hematoxylin, prior to mounting. Digital images were obtained at various magnifications (25 $\times$  to 200 $\times$ ) on a Zeiss Axiovert 40CFL microscope using AxioVision Release 4.6.3 digital imaging software (Carl Zeiss MicroImaging, Inc. Thornwood, NY).

## 2.9. Mechanical testing

For collagen scaffolds, a 12 mm  $\times$  12 mm square was cut from a central region of the cusp, with one edge aligned along the circumferential direction and another edge aligned along the radial direction ( $n = 5$ ). Similarly, a 12 mm  $\times$  12 mm square specimen was cut from the arterial scaffolds, maintaining orientation of the circumferential and longitudinal axes of the artery. The biaxial testing method has been reported previously [40]. Briefly, four markers were placed in the center of the specimen to track tissue deformation. A total of 8 loops of 000 polyester suture of equal length were attached to the sample via stainless steel hooks, with two loops on each side of the square specimen. Specimens were first preconditioned for 10 contiguous cycles, then loaded up to 60:60 N/m equibiaxial tension for collagen

scaffolds and 20:20 N/m tension for elastin scaffolds. Tissue extensibility was characterized by  $\lambda_{\text{circ}}$  and  $\lambda_{\text{rad}}$ , the maximum stretch ratio along the circumferential and radial directions, respectively. The biaxial testing was implemented with the samples completely immersed in PBS (pH 7.4) at physiological temperature (37  $^{\circ}\text{C}$ ).

## 2.10. Differential scanning calorimetry

To determine the thermal denaturation temperature ( $T_d$ ), also known as shrinkage temperature, a well-known indicator of collagen crosslinking [41], samples ( $n = 3$ ) were subjected to differential scanning calorimetry (DSC, model 131 Setaram Instrumentation, Caluire, France) at a heating rate of 10  $^{\circ}\text{C}/\text{min}$  from 20  $^{\circ}\text{C}$  to 110  $^{\circ}\text{C}$  in a  $\text{N}_2$  gas environment.  $T_d$  was defined as the temperature at the endothermic peak.

## 2.11. Detection of AGEs and MDA

N-epsilon-(carboxymethyl)lysine (CML) was detected by IHC, (ABC kit, Vector Laboratories). Briefly, rehydrated paraffin sections (5  $\mu\text{m}$ ,  $n = 4$  per group) were exposed to 0.1% Proteinase K in 10 mM Tris buffer, pH7.5, at room temperature for 30 s to unmask the antigens. Endogenous peroxidases were blocked with 0.3% hydrogen peroxide in 0.3% horse normal serum. Sections were treated with 0.025% Triton X-100 for 10 min and then incubated with normal blocking serum for 20 min. Primary antibody (4  $\mu\text{g}/\text{mL}$  mouse anti-CML) was applied for 1 h at room temperature. Rat-adsorbed biotinylated anti-mouse IgG was used as a secondary antibody. Negative staining controls were obtained by the omission of the primary antibody. The ABC peroxidase substrate kit was then used to visualize the antibody staining, and sections were lightly counterstained with Hematoxylin before mounting.

To detect and measure pentosidine and MDA in explanted scaffolds [9], tissues were weighed and their mass recorded. Samples were then incubated with collagenase type I (100 U/sample) in 50 mM HEPES buffer with 10 mM  $\text{CaCl}_2$ , pH = 7.5 at 37  $^{\circ}\text{C}$  until fully digested (2–4 days). Samples were then centrifuged for 10 min at 12000 rpm at 22  $^{\circ}\text{C}$  and the supernatant collected. Fluorescence of the supernatant was measured at 335/385 for pentosidine and at 390/460 for MDA [9] and expressed as relative fluorescence units per milligram original tissue wet weight.

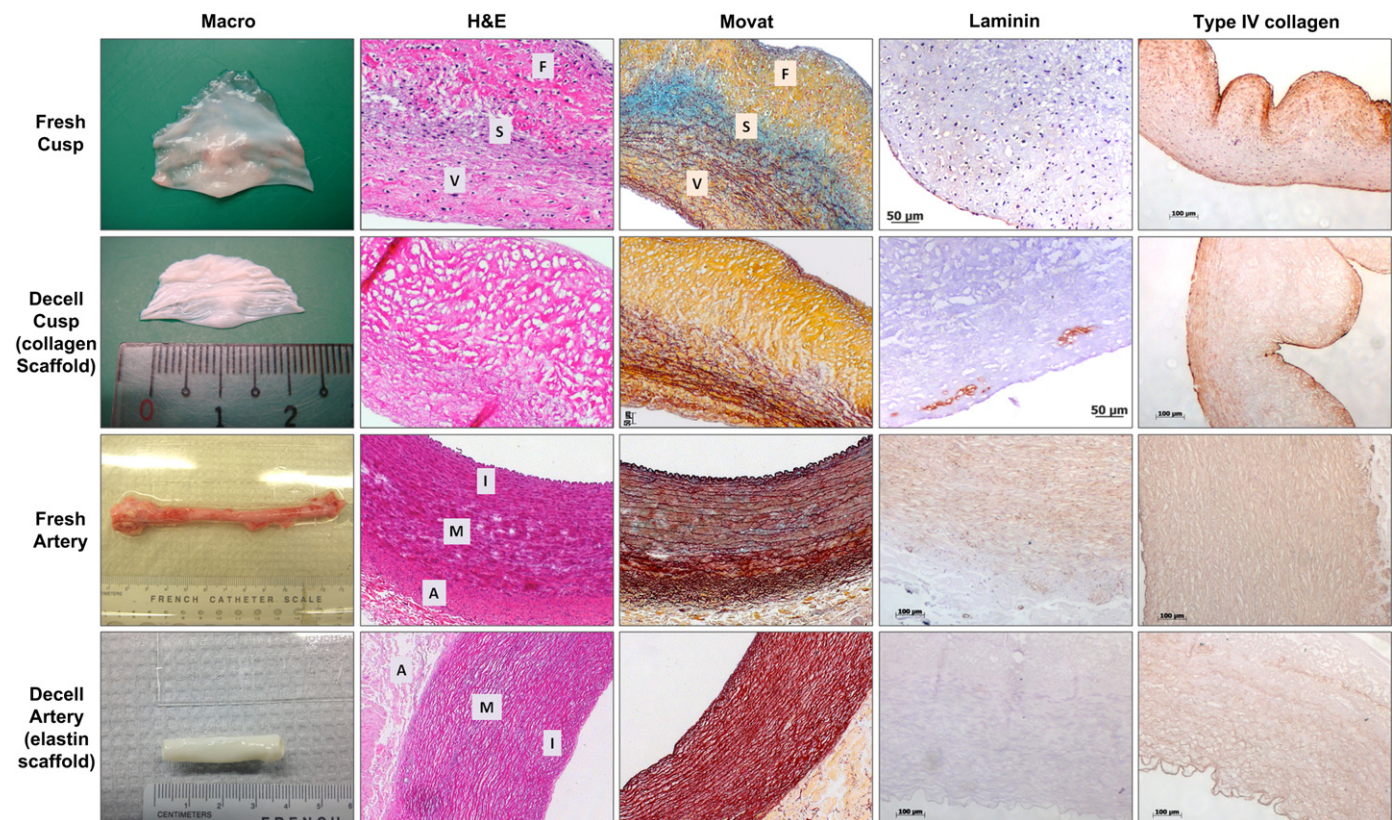


**Fig. 1.** Macroscopic and histological images of fresh and decellularized (decell) porcine aortic valve cusps (collagen scaffolds) and carotid arteries (elastin scaffolds) used in this study. For histological analysis, tissues were stained with Hematoxylin and Eosin (H&E, dark purple = nuclei, pink = background substance) and Movat's Pentachrome (yellow = collagen, blue = glycosaminoglycans, dark purple = elastin, bright red = nuclei). Tissues and scaffolds were also stained by immunohistochemistry for laminin and collagen type IV (brown = positive). Cusp layers: V = ventricularis, S = spongiosa, F = fibrosa. Arterial layers: I = intima, M = media, A = adventitia.

### 2.12. Evaluation of infiltrated cell phenotype

In order to identify the cells infiltrated in the scaffolds, we used IHC ( $n = 4$  samples per group), following the protocol described above for CML, and specific antibodies for fibroblasts (vimentin), T-lymphocytes (CD8) and macrophages (CD68).

### 2.13. MMP and TIMP detection

MMPs were detected in explanted scaffolds as described before [21]. Briefly, proteins were extracted by pulverizing liquid nitrogen-frozen tissue samples and homogenizing them in RIPA extraction buffer (50 mM Tris-HCl pH 7.4, 150 mM NaCl, 1 mM EDTA, 1% Triton X-100, 1% Sodium Deoxycholate, 0.1% SDS, with protease inhibitor cocktail). Protein concentration was determined using BCA assay. For each sample, 6  $\mu$ g per lane were loaded, alongside pre-stained molecular weight standards. After staining, the MMP clear bands on a dark background were evaluated by densitometry on a FluorChem SP imager and the Alpha EaseFC Software v. 4.1.0 by Alpha Innotech Corporation (Protein Simple, Santa Clara, CA) and expressed as relative density units normalized to protein content. Tissue inhibitors of MMPs (TIMP) levels were measured in the same protein extracts ( $n = 6$  per group, all 6 pooled into one assay sample) using a Rat Cytokine Array Panel (Proteome Profiler Antibody Array Panel A, R&D Systems, Minneapolis, MN).

### 2.14. Calcium analysis

Alizarin Red histology staining for calcium deposits was performed on sections of explanted scaffolds ( $n = 4$  per group) as described previously [37,42]. Calcium content was analyzed in tissue protein extracts ( $n = 4$  per group, see above method for MMP analysis) using a QuantiChrom Calcium Assay Kit (BioAssay Systems, Hayward, CA).

### 2.15. Statistical analysis

Results are expressed as means  $\pm$  standard deviation (SD). Statistical analysis was performed using one-way analysis of variance (ANOVA). Differences between means were determined using the least significant difference (LSD) with an alpha value of 0.05.

## 3. Results

### 3.1. Collagen and elastin scaffold characterization

Initial studies focused on characterization of the two scaffolds before pursuing implantation studies. Porcine aortic cusps and carotid arteries were chemically treated in order to remove all cells, but preserve the ECM components (methods of decellularization have been published by us previously [25,26]. As seen in Fig. 1, scaffolds showed complete elimination of cells (H&E staining); DNA analysis (agarose gel electrophoresis followed by densitometry, PicoGreen quantitative DNA assay, and Agilent Bioanalyzer lab-on-a-chip DNA kit) revealed complete DNA reduction after decellularization treatment in both tissues (results not shown). The scaffold exhibited typical "pores" (i.e. areas devoid of content where the original cells used to be), while maintaining most of the original matrix proteins, as confirmed by Movat's Pentachrome staining. In the cusp scaffolds, collagen predominated and was well preserved. Intact elastin fibers in the ventricularis layer were also visible. In

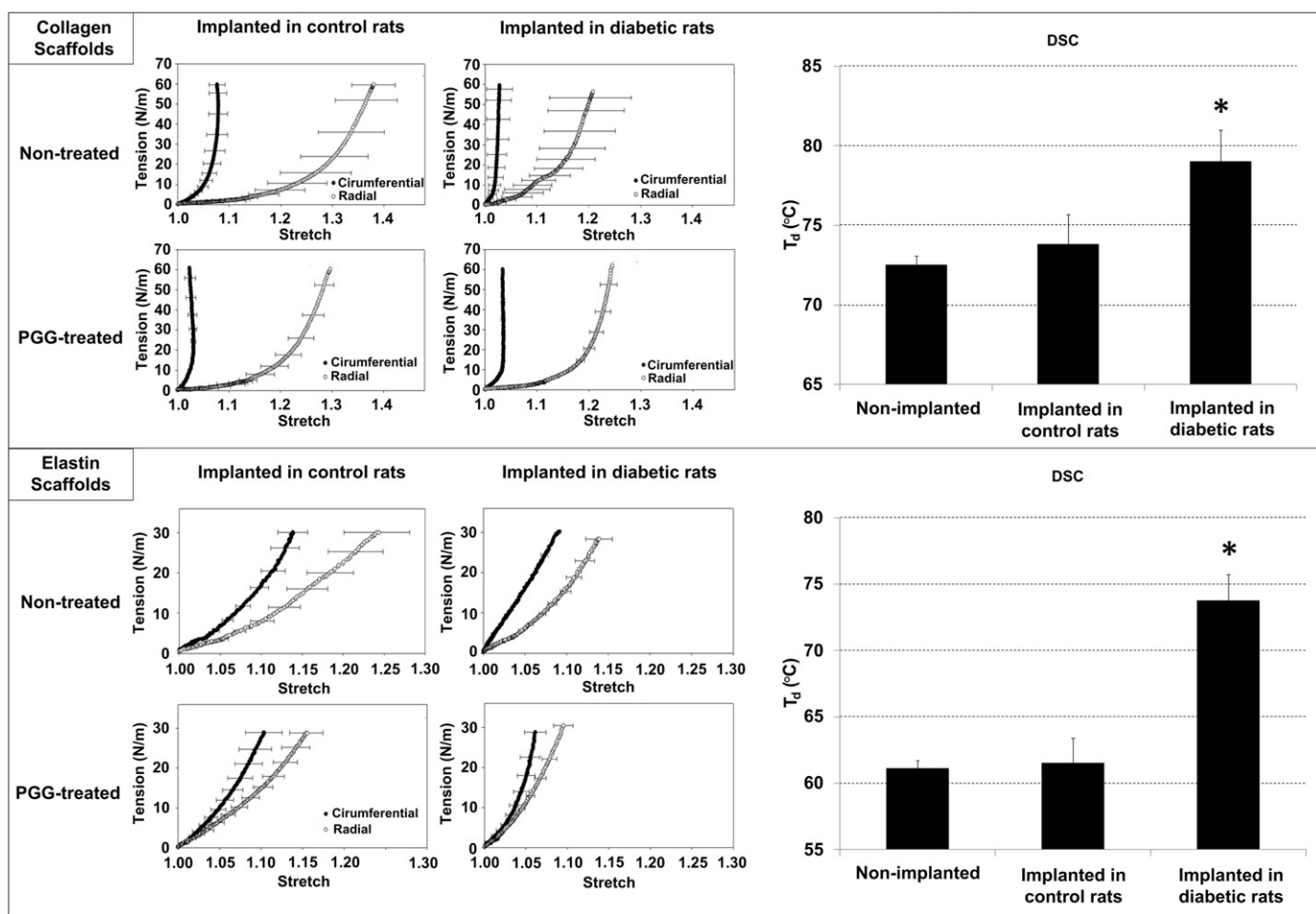


Fig. 2. Mechanical properties and matrix cross-linking in explanted scaffolds. Biaxial stress strain analysis showing tension vs. stretch plots, and differential scanning calorimetry (DSC) showing thermal denaturation temperatures ( $T_d$ ) of collagen scaffolds (top panel) and elastin scaffolds (bottom panel) after subdermal implantation in control rats and in diabetic rats. \*Indicates statistical significance.



the spongiosa layer, we noticed the loss of glycosaminoglycans. In the arterial scaffolds, elastin sheets were well preserved in all arterial tunics, while collagen was less visible (Fig. 1). IHC staining for basal lamina components revealed good preservation of collagen type IV in both scaffolds, while laminin showed only moderate retention in the cusp scaffolds.

### 3.2. Diabetes-related scaffold stiffening and crosslinking

Biaxial tensile test analysis showed that collagen and elastin scaffolds implanted in diabetic rats exhibited markedly increased stiffness in both radial and circumferential directions compared to scaffolds implanted into control (non-diabetic) rats (Fig. 2). Remarkably, PGG-treatment appeared to halt the pathological stiffening effect observed in scaffolds implanted into diabetic rats. Thus, there were no statistical differences in mechanical properties in either the radial or circumferential directions of PGG-treated acellular cusps and arteries implanted in diabetic rats as compared to their controls. Differential scanning calorimetry (DSC) showed significantly higher thermal denaturation temperatures

( $T_d$ ) of scaffolds explanted from diabetic environments (Fig. 2), strongly suggesting that diabetes induced stiffening and crosslink formation in collagen and elastin scaffolds.

### 3.3. Glycoxidation and lipid peroxidation

Having demonstrated that diabetes induced matrix protein crosslinking, we sought to further define diabetes-related changes in scaffolds implanted subdermally in diabetic rats. The presence of AGEs, specifically CML and pentosidine, and lipid peroxidation products such as MDA was demonstrated in implanted scaffolds (Fig. 3). Baseline levels of CML were detected by IHC in all scaffolds, regardless of glycemic conditions. Remarkably, CML antigen was highly expressed in non-PGG-treated scaffolds implanted in diabetic conditions, and was associated with both infiltrated host cells and the implanted extracellular matrix. However, PGG-treatment of the scaffolds before implantation markedly decreased the accumulation of CML in diabetic environments, particularly in the extracellular matrix (Fig. 3). Pentosidine and MDA detection in scaffold extracts essentially confirmed IHC results, showing that

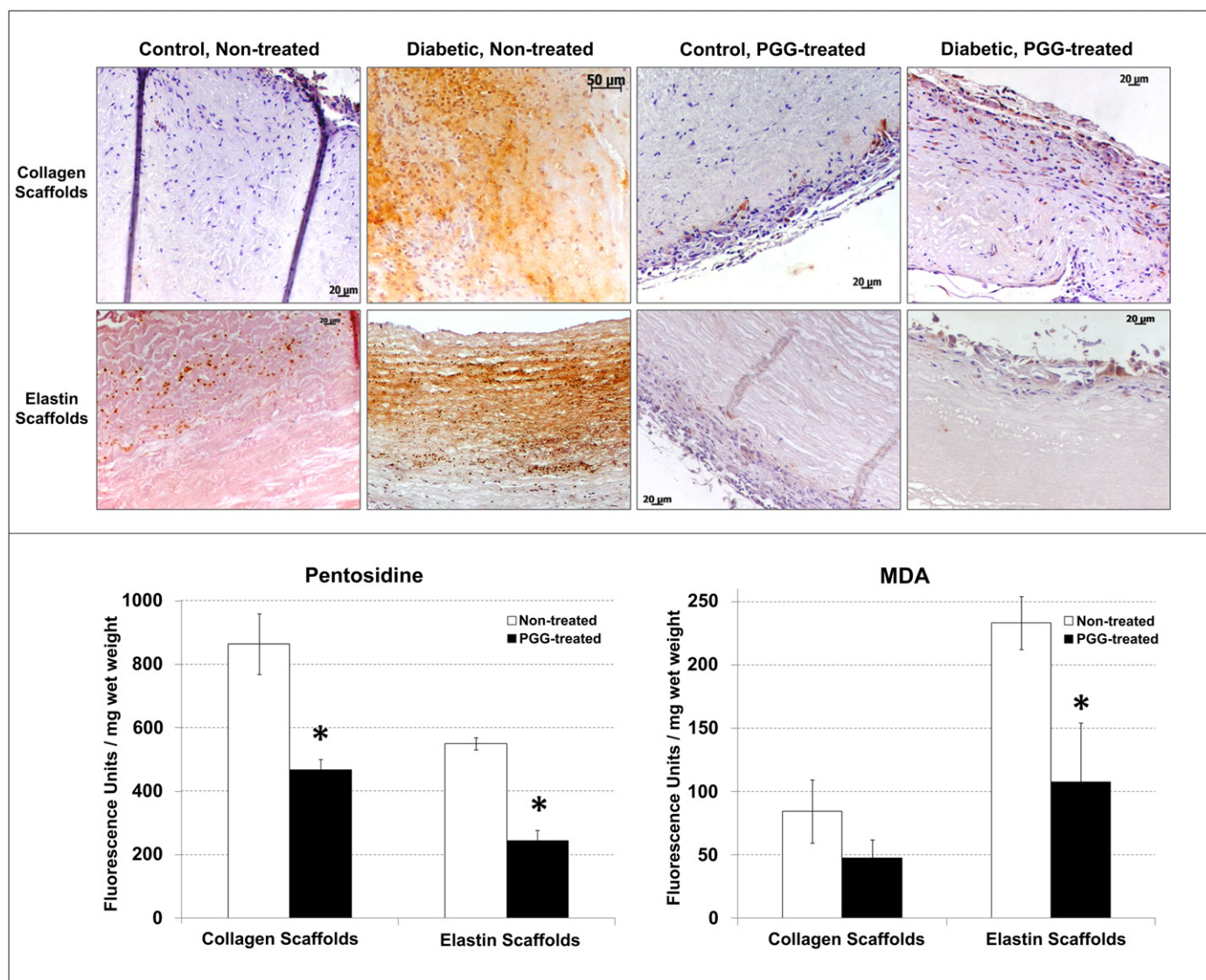


**Fig. 3.** Advanced glycation end products and lipid peroxidation products in explanted scaffolds. (top panel) Immunohistochemical detection of carboxymethyl lysine (CML) in non-treated and PGG-treated collagen and elastin scaffolds implanted in control and diabetic rats (positive = brown). (bottom panel) Pentosidine (left) and malondialdehyde (MDA, right) content in non-treated and PGG-treated collagen and elastin scaffolds after implantation in diabetic rats. \*Indicates statistical significance.



PGG-treated scaffolds allowed significantly less AGE formation and accumulation in diabetic environments when compared to non-PGG-treated scaffolds ( $p > 0.001$ ).

### 3.4. Cellular infiltration

In order to learn how the diabetic host cells react to the implanted collagen and elastin scaffolds and whether the treatment with PGG affects the inflammatory cell infiltration, we analyzed the scaffolds by H&E staining and IHC four weeks after implantation. H&E staining documented host cell infiltration permeating the scaffolds, preferentially through the ventricularis layer in the cusp and the adventitia in the artery (Figs. 4 and 5). Host cells appeared to have an affinity for the pore spaces in the collagen scaffolds and spaces between elastin fibers. No differences were observed in cell infiltration patterns between non-PGG-treated scaffolds implanted in diabetic rats as compared to those implanted in control, non-diabetic rats. PGG-treatment of scaffolds before implantation slightly reduced, but did not inhibit cellular infiltration.

IHC stain for vimentin documented an influx of fibroblasts into all scaffolds regardless of glycemic environments. Fibroblasts were seen to migrate throughout the scaffolds unhindered, and cell spreading was clearly seen in most areas analyzed. Treatment of scaffolds with PGG did not appear to inhibit fibroblast infiltration or spreading (Figs. 4 and 5). IHC for CD8 showed presence of few T-cells in all scaffolds, but they were constrained to the edges of the

scaffolds. Diabetic environments appeared to elicit a greater T-cell response in non-treated scaffolds compared with control non-treated scaffolds. PGG-treatment of scaffolds appeared to discourage T-cell infiltration, though it did not completely inhibit it. IHC staining for CD68 (a pan-macrophage antibody) showed presence of macrophages in all scaffolds, indicating an inflammatory response. This was noticeably more aggressive in diabetic non-treated scaffolds (Figs. 4 and 5). An evident decrease in general macrophage presence was observed in PGG-treated tissues, suggesting that PGG might discourage the macrophage inflammatory response of the host to the scaffolds.

### 3.5. ECM remodeling

Non-PGG-treated scaffold ECM integrity was slightly compromised after implantation, with signs of matrix degradation visible in both collagen and elastin scaffolds stained with Movat's Pentachrome (Fig. 6). Conversely, treatment of scaffolds with PGG before implantation preserved the structural integrity of the ECM in both control and diabetic conditions. Collagen and elastin scaffolds were also analyzed for MMP activities and amounts of TIMPs. Results showed higher MMP activities in diabetic vs. non-diabetic rats and significantly reduced protease levels in PGG-treated scaffolds. The highest reduction in MMP activity was noticed in PGG-treated scaffold samples implanted in diabetic rats (Fig. 6). TIMP levels were highest in non-PGG-treated scaffolds implanted in control, non-diabetic rats (0.27 RDU per mg wet weight) and lowest

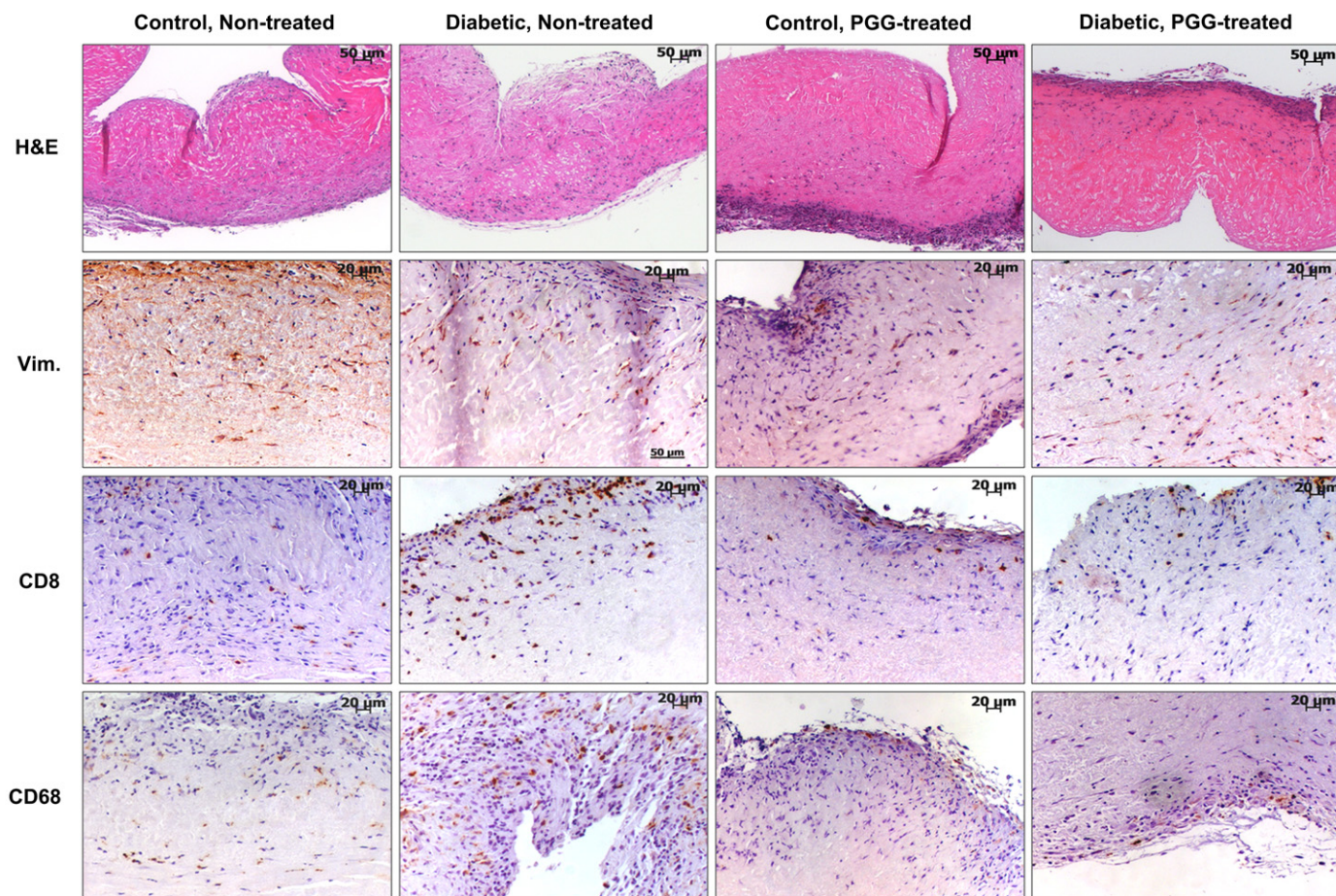


**Fig. 4.** Cell infiltration in collagen scaffolds. Decellularized porcine aortic valve cusps treated with PGG or non-treated controls were implanted subdermally in control and diabetic rats. Explants were stained by Hematoxylin and Eosin (H&E, dark purple = nuclei, pink = background substance) and immunohistochemistry for vimentin (Vim.), CD8 (T-lymphocytes) and CD68 (macrophages). Positive IHC reaction = brown. (For interpretation of the references to color in this figure legend, the reader is referred to the web version of this article.)



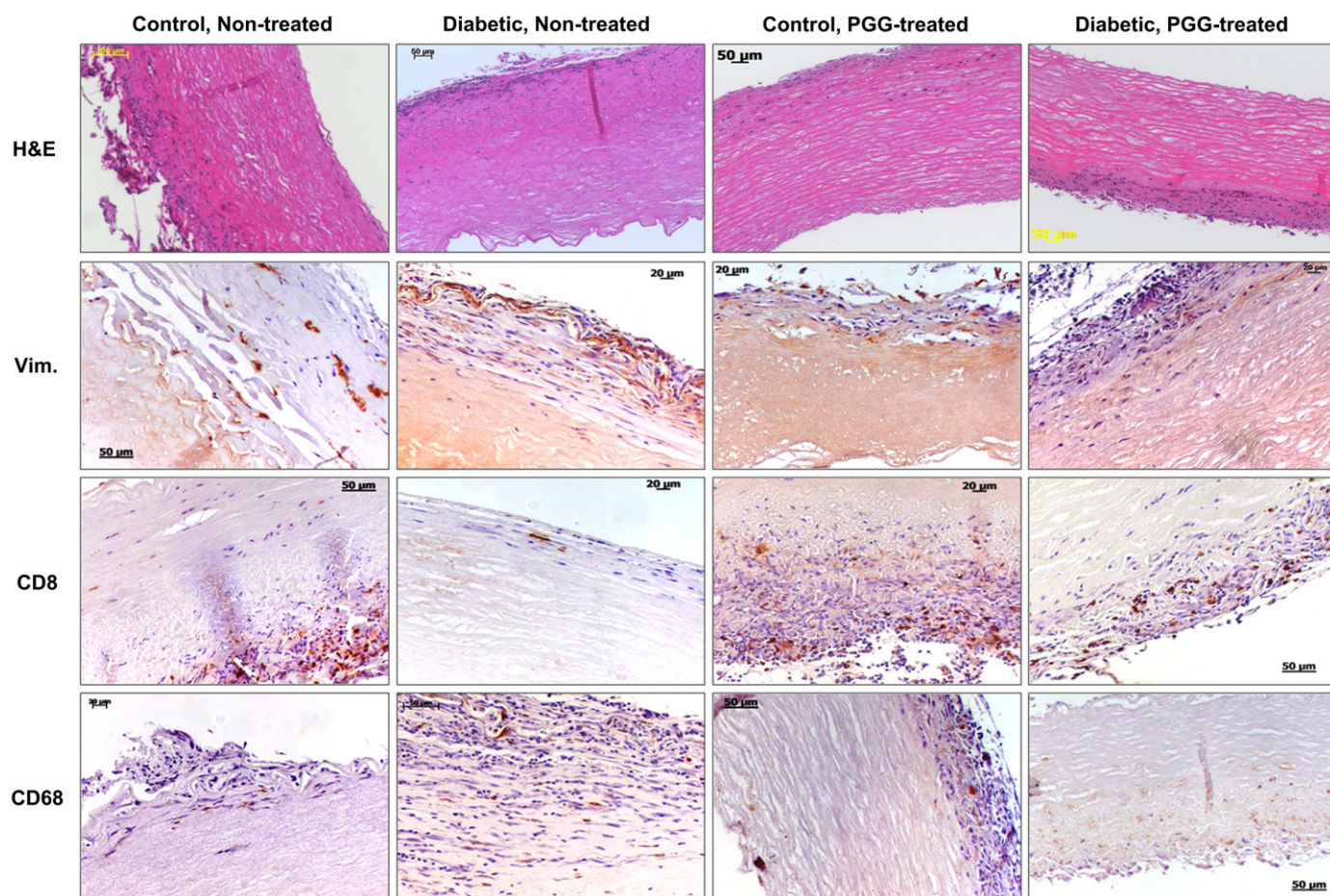


**Fig. 5.** Cell infiltration in elastin scaffolds. Decellularized porcine carotids treated with PGG or non-treated controls were implanted subdermally in control and diabetic rats. Explants were stained by Hematoxylin and Eosin (H&E, dark purple = nuclei, pink = background substance) and IHC for vimentin (Vim.), CD8 (T-lymphocytes) and CD68 (macrophages). Positive IHC reaction = brown. (For interpretation of the references to color in this figure legend, the reader is referred to the web version of this article.)

in PGG-treated scaffolds implanted in diabetic rats (0.19 RDU per mg wet weight).

### 3.6. Calcification

To test for calcification, samples from all groups were stained with Alizarin Red histological stain and also analyzed for calcium content using a colorimetric kit. Results revealed no accumulation of calcium in any of the collagen scaffolds (baseline levels of calcium) irrespective of glycemic status (Fig. 7). Elastin scaffolds however calcified significantly after being implanted in both normal and diabetic rats (17  $\mu\text{g}$  Ca/mg dry weight) but did not accumulate any calcium deposits if pre-treated with PGG before implantation (baseline levels, no red staining after Alizarin). These results point to important structural differences between the two scaffolds and the outstanding effect of PGG on elastin calcification.

## 4. Discussion

Biological scaffolds composed of ECM proteins have been used in numerous regenerative medicine applications, for both preclinical animal studies and clinical purposes [24,43]. The ECM is the natural 3D structure that assists the functions of cells and tissues, not only providing structural support for cells, but also regulating processes such as cell proliferation, survival, migration, and differentiation. Cell-matrix interactions constantly determine the remodeling of ECM superstructures during the normal processes of

development and wound repair. However, when cells detect and respond to altered matrix biochemical or mechanical stimuli from their environment, the dysfunctional remodeling that might occur can contribute to the onset and progression of disease [44]. One of the most daunting environments that could damage the ECM and its interaction with cells is progressively built in diabetes. In the presence of high glucose concentrations, long-lived ECM proteins such as collagen and elastin undergo irreversible crosslinking by the formation of AGEs through non-enzymatic glycation (Maillard reaction). Reactive oxygen species and free metal ions were identified as key participants in glycooxidation and lipid peroxidation processes [45]. Furthermore, AGEs interact with specific receptors on cell surfaces (RAGE), triggering continuous reactive oxygen species formation, inflammation, and progressive vascular complications [11]. The consequences of severe matrix alterations in diabetes are impaired healing, remodeling, and tissue regeneration, all being key processes targeted in tissue engineering and regenerative medicine.

In studies presented here, we show that matrix-based scaffolds used for heart valve and blood vessel tissue engineering accumulate AGEs, become crosslinked, change their mechanical and biochemical properties, trigger inflammatory reactions, and change their matrix remodeling abilities when subjected to experimentally induced diabetes in rats.

In order to prepare our collagen and elastin scaffolds, we developed suitable methods that remove all cells, but do not disturb the overall scaffold architecture [25,26]. Not only did the



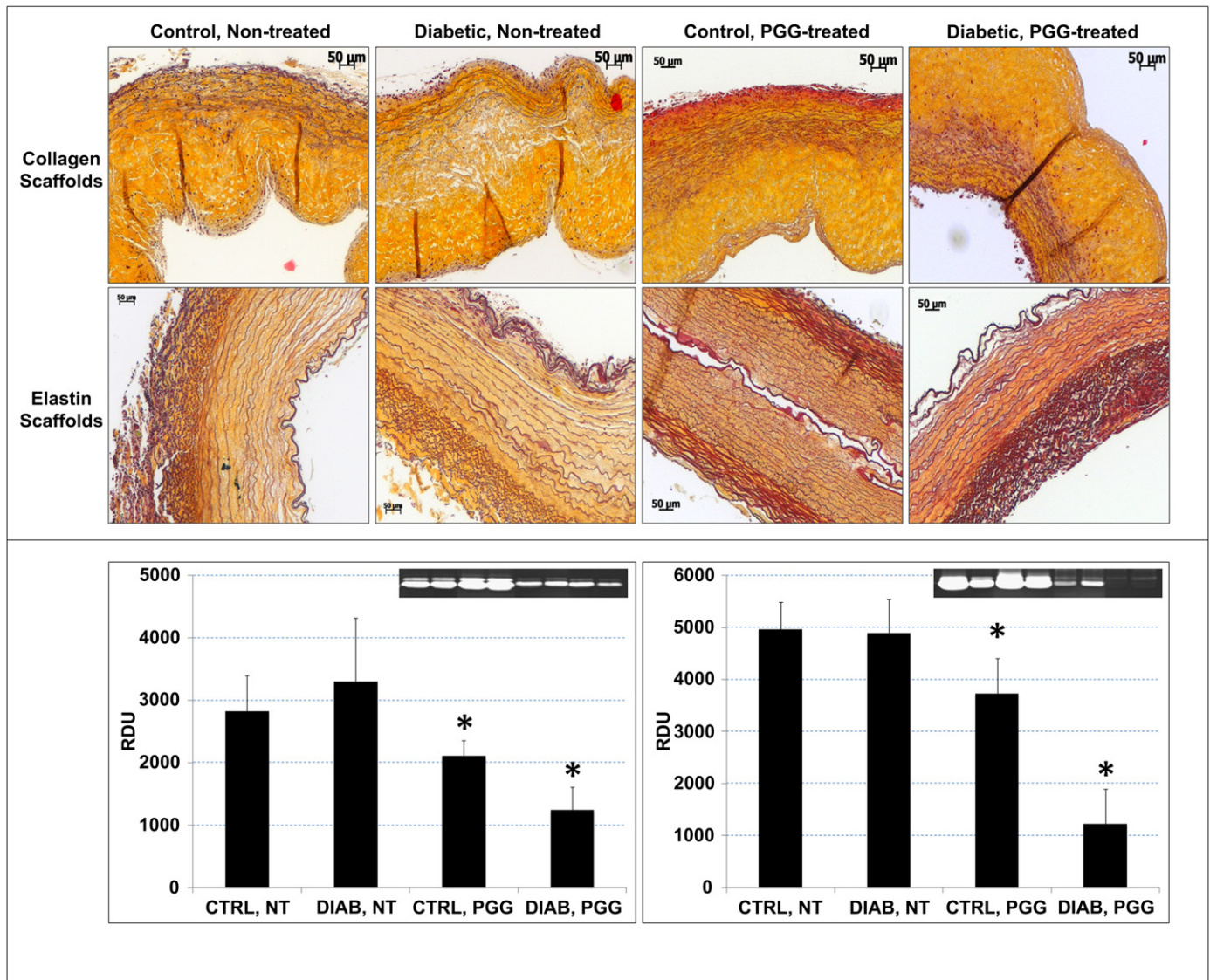


**Fig. 6.** ECM remodeling in implanted scaffolds. Scaffolds treated with PGG or non-treated controls were implanted subdermally in control and diabetic rats. (upper panel) Explants were stained with Movat's Pentachrome histology stain (yellow = collagen, blue = glycosaminoglycans, dark purple = elastin, bright red = nuclei). (bottom panel) Protein extracts from collagen scaffolds (left) and elastin scaffolds (right) were analyzed for matrix metalloproteinase activity by gelatin zymography followed by densitometry (inserts, positive = white bands); results are shown as relative density units (RDU). \*Indicates statistical significance. (For interpretation of the references to color in this figure legend, the reader is referred to the web version of this article.)

major collagen and elastin components of the ECM maintain their structures, but some basal lamina components, predominantly collagen type IV was also retained post-decellularization. Several studies have shown that if the basal lamina is not damaged, it provides a scaffold along which regenerating cells can migrate and regenerate injured tissues such as muscle, nerves, and epithelia [46–48]. Since the composition and architecture of the matrix are not compromised during decellularization, our scaffolds have similar mechanical properties compared to fresh tissues. These results are in agreement with several other studies that use decellularization methods which do not induce significant changes in the ECM composition vs. the native tissues and, consequently, do not impair tissue strength [29,49]. However, when implanted subcutaneously for four weeks in diabetic rats, both the collagen and the elastin scaffolds showed significantly altered mechanical properties, becoming stiffer, compared to those scaffolds implanted in non-diabetic surroundings. These physical changes are similar to

those already noticed in tissues obtained from diabetic patients. Without doubt, one of the most prominent complications of hyperglycemia is associated with the alteration of the vascular wall and, consequently, vascular stiffening is considered the hallmark of diabetes [50]. There is much ongoing research examining the mechanical properties of large and peripheral arteries in diseased states [51,52], with particular emphasis on the aorta [53]. However, there is currently little research examining mechanical properties of aortic valve cusps in a pathological state such as diabetes, although aortic valve cusp thickening and calcification were shown to be accelerated in diabetic patients, eventually ending in heavily calcified, stiff cusps causing severe valve stenosis [54,55].

We noticed in our animal studies that the diabetic environment elicited a pathological stiffening of collagen scaffolds, likely due to the crosslinking nature of AGEs. DSC confirmed the crosslinked nature of the scaffolds by illustrating an increased thermal denaturation temperature ( $T_d$ ) of 6–10 °C, which can be considered



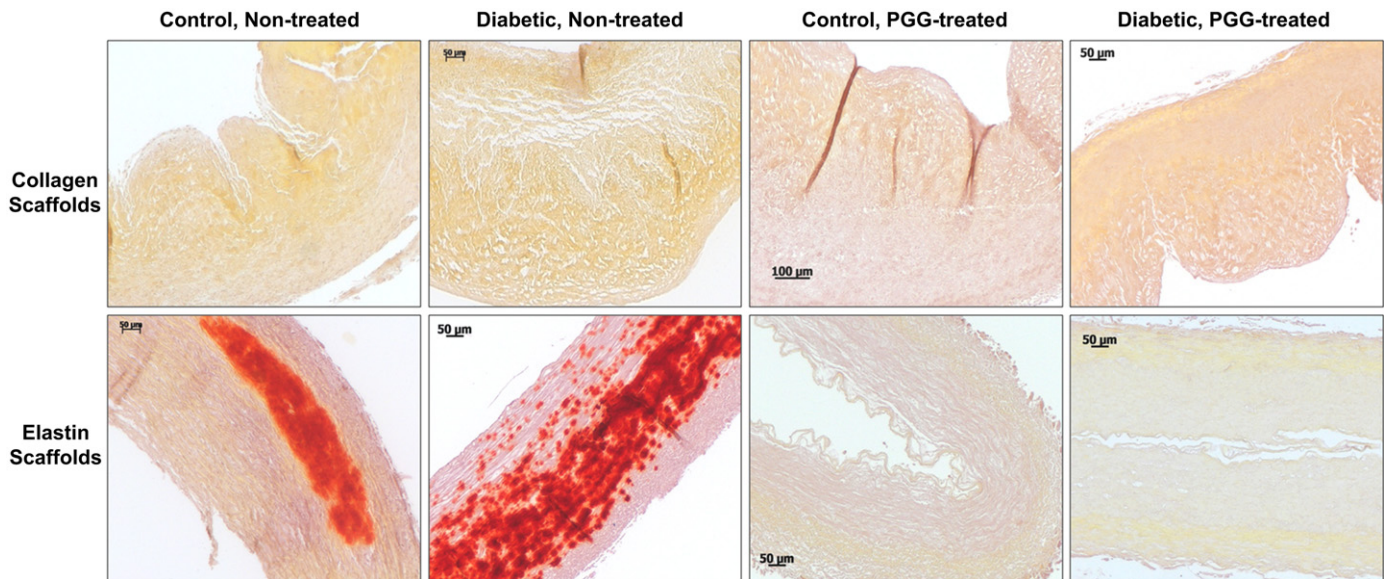


**Fig. 7.** Calcification in implanted scaffolds. Scaffolds treated with PGG or non-treated controls were implanted subdermally in control and diabetic rats. Explants were stained with Alizarin Red histology stain for calcium (positive = red).

significant. In fact, *in vitro* studies have also reported the formation of AGEs by  $\text{Fe}^{2+}$ -catalyzed, non-enzymatic glycosylation [8,56,57] of collagen type I incubated *in vitro* in solutions with high glucose concentrations.

As diabetes is increasing to epidemic proportions worldwide with severe consequences, numerous studies were performed to elucidate the nature of AGEs, their involvement in the generation of permanent crosslinks of extracellular matrix proteins, as well as their association with diabetes-induced complications. Concurrently, numerous studies are focused on finding effective means of attenuating the glucose adduct formation and the damage they are bringing to proteins [45]. Several strategies and agents were considered such as aspirin, glutathione, and dibasic aminoacids (lysine and arginine) to block glucose adduct formation: aminoguanidine and pyridoxamine [58], to trap the sugar fragmentation products; N-phenacylthiazolium bromide, to break AGEs; vitamin E and selenium, as agents with antioxidant supplements because the antioxidant defense system is perturbed in diabetes. As alterations in iron and copper homeostasis are a characteristic feature of diabetes, chelators, such as triethylenetetramine or citrate, may inhibit AGE formation [58].

A number of publications report on the protection against diabetic complications by several plant extracts, such as polyphenols, rutin [59], and resveratrol. It is possible that they may work in part by limiting the uptake or promoting the excretion of metal ions through chelating activities [58]. Given that high levels of CML, pentosidine and MDA were noticed in the collagen and elastin scaffolds exposed to the harmful environment in diabetic rats (Figs. 2 and 3), we treated our scaffolds with PGG, a polyphenolic, antioxidant stabilizing agent with high affinity for proline-rich proteins [60], and implanted them in diabetic rats. The reduced quantities of CML, pentosidine, and MDA in implanted PGG-treated collagen scaffolds compared to non-treated scaffolds suggest that PGG might protect cardiovascular tissue engineering scaffolds from diabetic complications.

It is known that inflammatory cells are often present in altered diabetic tissues [61]. Neutrophil, macrophage, and T-cell accumulation was also noticed in the collagen and elastin-based scaffolds implanted in diabetic rats. However, in the PGG-treated scaffolds, we noticed less cell infiltration. As there is a highly regulated

connection between AGEs, oxidative stress, and inflammation, it is possible that the antioxidant nature of PGG is halting the glyco-oxidation, which in turn, ceases the further acceleration of AGE accumulation and inflammation. These results are in agreement with other papers that describe PGG as an anti-inflammatory and anti-oxidative agent [39].

PGG was also efficient in preventing calcium accumulation in the elastin scaffolds. Many studies have demonstrated that elastin calcification is a widespread feature of vascular pathology [42,62,63] and that the glycooxidative modification of elastin is a potential accelerating factor for diabetic macroangiopathy [64,65]. In our studies, the acellular elastin scaffolds exhibited massive calcium deposits in the media after implantation in both control and diabetic rats. Auspiciously, the PGG-treated elastin scaffolds revealed no detectable calcium accumulation *in vivo*. These results were in agreement with studies done by Chuang et al., who showed that there were no detectable deposits of calcium salts at four weeks after subcutaneous implantation in normal rats [25]. In this study, we show that PGG is able to prevent calcification of elastin scaffolds in diabetic rats as well. Similarly, it was demonstrated earlier that tannic acid (a chemical derivative of PGG) decreased calcification of glutaraldehyde treated aorta implanted in the rat subdermal model [66]. The same authors revealed that stabilization of abdominal aorta with PGG reduced the onset and progression of abdominal aorta aneurysms and that PGG-treated aortas exhibited improved preservation of elastic lamellar integrity, waviness, and overall preserved tissue architecture in a well-established abdominal aortic aneurysm model in rats [37].

On the other hand, our collagen scaffolds were not readily susceptible to calcification upon four weeks implantation in diabetic rats, although studies have shown that diabetes is a strong predictor for aortic valve calcification [67]. The acellular collagen scaffolds proved to be resistant to calcification, possibly as a result of the mild detergent-based method that we used to decellularize the tissue (it has been shown that degraded collagen fibers are associated with valve calcification) [68,69]. In addition, PGG might prevent the further disorganization of matrix components, reducing the infiltration of inflammatory cells and the synthesis of matrix proteases, which play a significant role in elastin and collagen calcification [42]. The activity of MMPs was slightly higher

in scaffolds implanted in diabetic rats, compared to non-diabetic rats; as expected, TIMP levels were lower in diabetic conditions. These results are in agreement with studies that show that both MMP activities and TIMP protein levels are altered in different cell types isolated from diabetic patients [12]. In our scaffolds, MMP levels were about 50% lower in PGG-treated scaffolds implanted in both non-diabetic and diabetic rats. This indicates that the remodeling process would be likely decelerated, allowing prolonged scaffold retention, an essential characteristic for use in replacement of cardiovascular tissues.

## 5. Conclusions

Collagen and elastin - based scaffolds used for heart valve and blood vessel tissue engineering accumulate AGEs, become stiffer, and change their matrix remodeling abilities when subjected to experimentally induced diabetes in rats. Pre-implantation treatment of scaffolds with PGG, an antioxidant matrix-binding polyphenol, stabilizes the scaffolds and protects them from diabetes-related complications thereby supporting their future use for cardiovascular tissue engineering in diabetic patients.

## Acknowledgments

The authors wish to acknowledge the Godley Snell Research Center animal facility for help with the animal studies. This work was funded by NIH grant 1R21EB009835-01A1 (to A.Simionescu).

## References

- [http://www.cdc.gov/diabetes/pubs/pdf/ndfs\\_2011.pdf](http://www.cdc.gov/diabetes/pubs/pdf/ndfs_2011.pdf).
- Goldberg RB. Cardiovascular disease in patients who have diabetes. *Cardiol Clin* 2003;21(3):399–413. vii.
- Briand M, Lemieux I, Dumesnil JG, Mathieu P, Cartier A, Despres JP, et al. Metabolic syndrome negatively influences disease progression and prognosis in aortic stenosis. *J Am Coll Cardiol* 2006;47(11):2229–36.
- Messika-Zeitoun D, Bielak LF, Peyser PA, Sheedy PF, Turner ST, Nkomo VT, et al. Aortic valve calcification: determinants and progression in the population. *Arterioscler Thromb Vasc Biol* 2007;27(3):642–8.
- Peterson LR, McKenzie CR, Schaffer JE. Diabetic cardiovascular disease: getting to the heart of the matter. *J Cardiovasc Transl Res* 2012;5(4):436–45.
- Winlove CP, Parker KH, Avery NC, Bailey AJ. Interactions of elastin and aorta with sugars in vitro and their effects on biochemical and physical properties. *Diabetologia* 1996;39(10):1131–9.
- Sakata N, Noma A, Yamamoto Y, Okamoto K, Meng J, Takebayashi S, et al. Modification of elastin by pentosidine is associated with the calcification of aortic media in patients with end-stage renal disease. *Nephrol Dial Transplant* 2003;18(8):1601–9.
- Meli M, Granouillet R, Reynaud E, Chamson A, Frey J, Perier C. In vitro glyco-oxidation of insoluble fibrous type I collagen: solubilization and advanced glycation end products. *J Protein Chem* 2003;22(6):527–31.
- Sakuda S, Tamura S, Yamada A, Miyagawa J, Yamamoto K, Kiso S, et al. NF- $\kappa$ B activation in non-parenchymal liver cells after partial hepatectomy in rats: possible involvement in expression of heparin-binding epidermal growth factor-like growth factor. *J Hepatol* 2002;36(4):527–33.
- Nagai R, Murray DB, Metz TO, Baynes JW. Chelation: a fundamental mechanism of action of AGE inhibitors, AGE breakers, and other inhibitors of diabetes complications. *Diabetes* 2012;61(3):549–59.
- Negre-Salvayre A, Salvayre R, Auge N, Pamplona R, Portero-Otin M. Hyperglycemia and glycation in diabetic complications. *Antioxid Redox Signal* 2009;11(12):3071–109.
- Tayebjee MH, Lip GY, MacFadyen RJ. What role do extracellular matrix changes contribute to the cardiovascular disease burden of diabetes mellitus? *Diabet Med* 2005;22(12):1628–35.
- Huebschmann AG, Regensteiner JG, Vlassara H, Reusch JE. Diabetes and advanced glycooxidation end products. *Diabetes Care* 2006;29(6):1420–32.
- Nguyen LL. Percutaneous treatment of peripheral vascular disease: the role of diabetes and inflammation. *J Vasc Surg* 2007;45(Suppl. A):A149–57.
- Nugent HM, Edelman ER. Tissue engineering therapy for cardiovascular disease. *Circ Res* 2003;92(10):1068–78.
- Mensah GA, Catravas JD, Engelgau MM, Hooper WC, Madeddu P, Ryan US, et al. Vascular endothelium summary statement VI: research directions for the 21st century. *Vasc Pharmacol* 2007;46(5):330–2.
- Krawiec JT, Vorp DA. Adult stem cell-based tissue engineered blood vessels: a review. *Biomaterials* 2012;33(12):3388–400.
- Peck M, Gebhart D, Dusserre N, McAllister TN, L'Heureux N. The evolution of vascular tissue engineering and current state of the art. *Cells Tissues Organs* 2012;195(1–2):144–58.
- Iseberg BC, Williams C, Tranquillo RT. Small-diameter artificial arteries engineered in vitro. *Circ Res* 2006;98(1):25–35.
- Schoen FJ. Heart valve tissue engineering: quo vadis? *Curr Opin Biotechnol* 2011;22(5):698–705.
- Tedder ME, Simionescu A, Chen J, Liao J, Simionescu DT. Assembly and testing of stem cell-seeded layered collagen constructs for heart valve tissue engineering. *Tissue Eng Part A* 2011;17(1–2):25–36.
- Iyer RK, Chiu LL, Reis LA, Radisic M. Engineered cardiac tissues. *Curr Opin Biotechnol* 2011;22(5):706–14.
- Bursac N, Papadaki M, White JA, Eisenberg SR, Vunjak-Novakovic G, Freed LE. Cultivation in rotating bioreactors promotes maintenance of cardiac myocyte electrophysiology and molecular properties. *Tissue Eng* 2003;9(6):1243–53.
- Badylak SF. The extracellular matrix as a biologic scaffold material. *Biomaterials* 2007;28(25):3587–93.
- Chuang TH, Stabler C, Simionescu A, Simionescu DT. Polyphenol-stabilized tubular elastin scaffolds for tissue engineered vascular grafts. *Tissue Eng Part A* 2009;15(10):2837–51.
- Sierad LN, Simionescu A, Albers C, Chen J, Maivelett J, Tedder ME, et al. Design and testing of a pulsatile conditioning system for dynamic endothelialization of polyphenol-stabilized tissue engineered heart valves. *Cardiovasc Eng Technol* 2010;1(2):138–53.
- Barnes CA, Brison J, Michel R, Brown BN, Castner DG, Badylak SF, et al. The surface molecular functionality of decellularized extracellular matrices. *Biomaterials* 2011;32(1):137–43.
- Jiao T, Clifton RJ, Converse GL, Hopkins RA. Measurements of the effects of decellularization on viscoelastic properties of tissues in ovine, baboon, and human heart valves. *Tissue Eng Part A* 2012;18(3–4):423–31.
- Dahan N, Zarbiv G, Sarig U, Karram T, Hoffman A, Machluf M. Porcine small diameter arterial extracellular matrix supports endothelium formation and media remodeling forming a promising vascular engineered biograft. *Tissue Eng Part A* 2012;18(3–4):411–22.
- Cummings I, George S, Kelm J, Schmidt D, Emmert MY, Weber B, et al. Tissue-engineered vascular graft remodeling in a growing lamb model: expression of matrix metalloproteinases. *Eur J Cardiothorac Surg* 2012;41(1):167–72.
- Henriksen EJ, Diamond-Stanic MK, Marchionne EM. Oxidative stress and the etiology of insulin resistance and type 2 diabetes. *Free Radic Biol Med* 2011;51(5):993–9.
- Rees DA, Alcolado JC. Animal models of diabetes mellitus. *Diabet Med* 2005;22(4):359–70.
- Styskal J, Van Remmen H, Richardson A, Salmon AB. Oxidative stress and diabetes: what can we learn about insulin resistance from antioxidant mutant mouse models? *Free Radic Biol Med* 2012;52(1):46–58.
- Dobrev MA, Frazier RA, Mueller-Harvey I, Clifton LA, Gea A, Green RJ. Binding of pentagalloyl glucose to two globular proteins occurs via multiple surface sites. *Biomacromolecules* 2011;12(3):710–5.
- Tedder ME, Liao J, Weed B, Stabler C, Zhang H, Simionescu A, et al. Stabilized collagen scaffolds for heart valve tissue engineering. *Tissue Eng Part A* 2009;15(6):1257–68.
- Iseberg JC, Karamchandani NV, Simionescu DT, Vyavahare NR. Structural requirements for stabilization of vascular elastin by polyphenolic tannins. *Biomaterials* 2006;27(19):3645–51.
- Iseberg JC, Simionescu DT, Starcher BC, Vyavahare NR. Elastin stabilization for treatment of abdominal aortic aneurysms. *Circulation* 2007;115(13):1729–37.
- Ren Y, Himmeldirk K, Chen X. Synthesis and structure-activity relationship study of anti-diabetic penta-O-galloyl-D-glucopyranose and its analogues. *J Med Chem* 2006;49(9):2829–37.
- Zhang J, Li L, Kim SH, Hagerman AE, Lu J. Anti-cancer, anti-diabetic and other pharmacologic and biological activities of penta-galloyl-glucose. *Pharm Res* 2009;26(9):2066–80.
- Liao J, Joyce EM, Sacks MS. Effects of decellularization on the mechanical and structural properties of the porcine aortic valve leaflet. *Biomaterials* 2008;29(8):1065–74.
- Kasyanov V, Iseberg J, Draughn RA, Hazard S, Hodde J, Ozolanta I, et al. Tannic acid mimicking dendrimers as small intestine submucosa stabilizing nanomordants. *Biomaterials* 2006;27(5):745–51.
- Basalyga DM, Simionescu DT, Xiong W, Baxter BT, Starcher BC, Vyavahare NR. Elastin degradation and calcification in an abdominal aorta injury model: role of matrix metalloproteinases. *Circulation* 2004;110(22):3480–7.
- Badylak SF, Freytes DO, Gilbert TW. Extracellular matrix as a biological scaffold: structure and function. *Acta Biomater* 2009;5(1):1–13.
- Daley WP, Peters SB, Larsen M. Extracellular matrix dynamics in development and regenerative medicine. *J Cell Sci* 2008;121(Pt 3):255–64.
- Reiser KM. Nonenzymatic glycation of collagen in aging and diabetes. *Proc Soc Exp Biol Med* 1998;218(1):23–37.
- Chen X, Li Y. Role of matrix metalloproteinases in skeletal muscle: migration, differentiation, regeneration and fibrosis. *Cell Adh Migr* 2009;3(4):337–41.
- La Fleur M, Underwood JL, Rappolee DA, Werb Z. Basement membrane and repair of injury to peripheral nerve: defining a potential role for macrophages, matrix metalloproteinases, and tissue inhibitor of metalloproteinases-1. *J Exp Med* 1996;184(6):2311–26.



- [48] Albera C, Polak JM, Janes S, Griffiths MJ, Alison MR, Wright NA, et al. Repopulation of human pulmonary epithelium by bone marrow cells: a potential means to promote repair. *Tissue Eng* 2005;11(7–8):1115–21.
- [49] Korossis SA, Wilcox HE, Watterson KG, Kearney JN, Ingham E, Fisher J. In-vitro assessment of the functional performance of the decellularized intact porcine aortic root. *J Heart Valve Dis* 2005;14(3):408–21. discussion 422.
- [50] Martens FM, van der Graaf Y, Dijk JM, Olijhoek JK, Visseren FL. Carotid arterial stiffness is marginally higher in the metabolic syndrome and markedly higher in type 2 diabetes mellitus in patients with manifestations of arterial disease. *Atherosclerosis* 2008;197(2):646–53.
- [51] Soldatos G, Jandeleit-Dahm K, Thomson H, Formosa M, D'Orsa K, Calkin AC, et al. Large artery biomechanics and diastolic dysfunction in patients with type 2 diabetes. *Diabet Med* 2011;28(1):54–60.
- [52] Webb DR, Khunti K, Silverman R, Gray LJ, Srinivasan B, Lacy PS, et al. Impact of metabolic indices on central artery stiffness: independent association of insulin resistance and glucose with aortic pulse wave velocity. *Diabetologia* 2010;53(6):1190–8.
- [53] Karamitsos TD, Karvounis HI, Didangelos TP, Papadopoulos CE, Dalamanga EG, Karamitsos DT, et al. Usefulness of colour tissue doppler imaging in assessing aortic elastic properties in type 1 diabetic patients. *Diabetic Med* 2006;23(11):1201–6.
- [54] Rosenhek R, Baumgartner H. Aortic sclerosis, aortic stenosis and lipid-lowering therapy. *Expert Rev Cardiovasc Ther* 2008;6(3):385–90.
- [55] Falcao-Pires I, Hamdani N, Borbely A, Gavina C, Schalkwijk CG, van der Velden J, et al. Diabetes mellitus worsens diastolic left ventricular dysfunction in aortic stenosis through altered myocardial structure and cardiomyocyte stiffness. *Circulation* 2011;124(10):1151–9.
- [56] Xiao H, Cai G, Liu M. Fe<sup>2+</sup>-catalyzed non-enzymatic glycosylation alters collagen conformation during AGE-collagen formation in vitro. *Arch Biochem Biophys* 2007;468(2):183–92.
- [57] Meli M, Granouillet OR, Reynaud E, Chamson A, Frey J, Perier C. Changes in glycation of fibrous type I collagen during long-term in vitro incubation with glucose. *J Protein Chem* 2003;22(6):521–5.
- [58] Alt N, Carson JA, Alderson NL, Wang Y, Nagai R, Henle T, et al. Chemical modification of muscle protein in diabetes. *Arch Biochem Biophys* 2004;425(2):200–6.
- [59] Cervantes-Laurean D, Schramm DD, Jacobson EL, Halaweish I, Bruckner GG, Boissonneault GA. Inhibition of advanced glycation end product formation on collagen by rutin and its metabolites. *J Nutr Biochem* 2006;17(8):531–40.
- [60] Charlton AJ, Baxter NJ, Khan ML, Moir AJ, Haslam E, Davies AP, et al. Polyphenol/peptide binding and precipitation. *J Agric Food Chem* 2002;50(6):1593–601.
- [61] Galkina E, Ley K. Leukocyte recruitment and vascular injury in diabetic nephropathy. *J Am Soc Nephrol* 2006;17(2):368–77.
- [62] Sage AP, Tintut Y, Demer LL. Regulatory mechanisms in vascular calcification. *Nat Rev Cardiol* 2010;7(9):528–36.
- [63] Bostrom KI, Rajamannan NM, Towler DA. The regulation of valvular and vascular sclerosis by osteogenic morphogens. *Circ Res* 2011;109(5):564–77.
- [64] Edmonds ME. Medial arterial calcification and diabetes mellitus. *Z Kardiol* 2000;89(Suppl. 2):101–4.
- [65] Lehto S, Niskanen L, Suhonen M, Ronnema T, Laakso M. Medial artery calcification. A neglected harbinger of cardiovascular complications in non-insulin-dependent diabetes mellitus. *Arterioscler Thromb Vasc Biol* 1996;16(8):978–83.
- [66] Isenburg JC, Simionescu DT, Vyavahare NR. Tannic acid treatment enhances biostability and reduces calcification of glutaraldehyde fixed aortic wall. *Biomaterials* 2005;26(11):1237–45.
- [67] Katz R, Wong ND, Kronmal R, Takasu J, Shavelle DM, Probstfield JL, et al. Features of the metabolic syndrome and diabetes mellitus as predictors of aortic valve calcification in the multi-ethnic study of atherosclerosis. *Circulation* 2006;113(17):2113–9.
- [68] Gu X, Masters KS. Regulation of valvular interstitial cell calcification by adhesive peptide sequences. *J Biomed Mater Res A* 2010;93(4):1620–30.
- [69] Simionescu A, Schulte JB, Fercana G, Simionescu DT. Inflammation in cardiovascular tissue engineering: the challenge to a promise: a minireview. *Int J Inflamm* 2011. 2011958247.